Prolyl hydroxylase inhibition during hyperoxia prevents oxygen-induced retinopathy

Jonathan E. Sears[a,b,1], George Hoppe[a], Quteba Ebrahem[a], and Bela Anand-Apte[a,b]

Departments of [a]Ophthalmic Research and [b]Cell Biology, Cleveland Clinic Lerner College of Medicine, Cleveland Clinic Foundation, Cleveland OH 44195

Oxygen-induced retinopathy (OIR) in the mouse, like the analogous human disease retinopathy of prematurity, is an ischemic retinopathy dependent on oxygen-induced vascular obliteration. We tested the hypothesis that chemically overriding the oxygen-induced downregulation of hypoxia-inducible factor (HIF) activity would prevent vascular obliteration and subsequent pathologic neovascularization in the OIR model. Because the degradation of HIF-1α is regulated by prolyl hydroxylases, we examined the effect of systemic administration of a prolyl hydroxylase inhibitor, dimethyloxalylglycine, in the OIR model. Our results determine that stabilizing HIF activity in the early phase of OIR prevents the oxygen-induced central vessel loss and subsequent vascular tortuosity and tufting that is characteristic of OIR. Overall, these findings imply that simulating hypoxia chemically by stabilizing HIF activity during the causative ischemia phase (hyperoxia) of retinopathy of prematurity may be of therapeutic value in preventing progression to the proliferative stage of the disease.

dimethyloxalylglycine | erythropoeitin | hypoxia-inducible factor | retinopathy of prematurity | vascular endothelial growth factor

Retinopathy of prematurity (ROP) is a retinovascular disease of severely premature infants characterized by neovascularization at the intersection of developed, vascularized retina and undeveloped avascular retina. ROP has two phases, based on the oxygen-regulated expression of VEGF (1, 2). Phase I begins at birth when the infant is placed into hyperoxia, which results in a reduction in the secretion of VEGF that is associated with oxygen-induced vascular obliteration. Phase II is a hypoxic state created by weaning of oxygen supplementation and increased retinal metabolic demand exacerbated by vessel loss from phase I. Phase II is characterized by an overexpression of growth factors, such as VEGF, from the ischemic retina, resulting in pathologic neovascularization. The central roles that hyperoxia and hypoxia play in the development of ROP suggest a critical need for studying the role of oxygen and oxygen-regulated transcription factors such as hypoxia-inducible factor (HIF), their relationship to ischemia, and the subsequent development of the disease. Although much attention has been focused on the treatment of the angiogenic phase by VEGF and HIF inhibitors (3–5), we hypothesized that preventing the oxygen-induced downregulation of HIF in the initial phase of ROP would result in a protective effect and loss of progression to the angiogenic phase II of the disease.

HIF-1, and its related isoform HIF-2, are multimeric oxygen-regulated transcription factors critical to vascular development and maintenance (6, 7). HIF-1 and -2 are homologous heterodimers composed of inducible α and constitutive β subunits (8, 9). The stability of HIF-1α is regulated by prolyl hydroxylases (PHD), which induce hydroxylation on two proline residues (Pro-402 and Pro-564) within the oxygen degradation domain (ODD) (10, 11). This enables the interaction of the von Hippel-Lindau protein with the ODD to promote ubiquitination and degradation in the 26S proteasome (12). Inhibition of PHD can be induced by oxoglutarate analogues, such as dimethyloxalylglycine (DMOG), which competitively inhibit the hydroxylation of HIF-1/2α by displacing the endogenous oxoglutarate cofactor

(13, 14). Lack of hydroxylation of HIF-1/2 in the oxygen degradation domain results in prevention of degradation and increased stability of HIF-1α and -2α (11, 15), allowing them to dimerize with their respective β subunits to form the active HIF complex.

We tested the hypothesis that activating HIF during the hyperoxic phase of ROP would allow for normal retinovascular development and prevent the development of the hypoxia-induced neovascularization and phase II of the disease.

Results

Inhibition of PHD Induces Expression of HIF-1α and HIF-2α. To determine whether DMOG, an inhibitor of PHD, could stabilize HIF-1α and HIF-2α, cultured human retinal Müller cells were exposed to increasing concentrations of DMOG. Inhibition of PHD resulted in an increase in both HIF-1α and HIF-2α to similar levels as that induced by hypoxia-mimetics cobalt and desferrioxamine (Fig. 1).

Activation of HIF in the Hyperoxic Phase Prevents Oxygen-Induced Retinopathy. Systemic injection of the HIF activator DMOG in phase I of oxygen-induced retinopathy (OIR) (Fig. 2, blue arrows) at postnatal day 6 (P6) and 8 (P8) resulted in a dramatic inhibition of OIR pathology (Fig. 3A, control; Fig. 3B, DMOG treated). A significant decrease in capillary drop-out ($P = 0.004$), vascular tortuosity ($P = 0.043$), and tufting ($P = 5.7 \times 10^{-7}$) (Fig. 3D) was observed in mice treated with DMOG (200 μg/g body weight) during the hyperoxic phase when compared with control (PBS)-injected animals. As expected, administration of DMOG during the hypoxic phase II of OIR (Fig. 2, red arrows) at P11 and P13 did not induce this protective effect (Fig. 3E, control; Fig. 3F, DMOG treated). Statistical analysis of phase II injection (Fig. 3H) showed no difference between control- and DMOG-injected animals. A typical overlay used to quantitate the vascular parameters is displayed in Fig. 3G, and high magnification of the vascular tufts is shown in Fig. 3C. To determine whether administration of the HIF activator during phase I prevented OIR by inhibiting hyperoxia-induced vascular obliteration, we tested whether hypoxic preconditioning of mouse pups at P6, which should activate HIF, had a similar protective effect. Mouse pups were exposed to 10% O_2 (hypoxia) for 24 h or injected with HIF activator at P6 and placed in a hyperoxic chamber for 3 days. Retinas were examined at P10 for central vascular obliteration and vessel tortuosity. The bar graph in Fig. 4 shows the difference in capillary drop-out or avascularity between control (PBS injected) and i.p. DMOG. The preservation of capillaries in the posterior pole in pups subjected to hypoxic preconditioning (Fig. 4A) as well as DMOG injections (Fig. 4D) when compared with nonpreconditioned (Fig. 4B) and
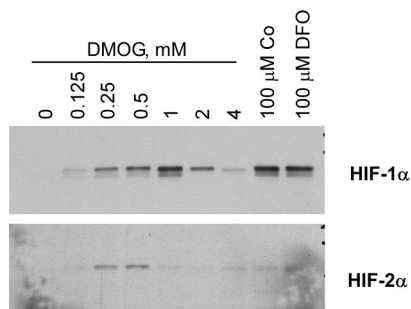
Fig. 1. Stabilization of HIF by DMOG in Müller cells. Cultured human Müller cells were exposed to increasing concentrations of DMOG for 24 h, and cells were harvested and subjected to Western blotting using HIF-1α (*Top*) and HIF-2α (*Bottom*) antibodies. Lanes 8 and 9 are positive controls using hypoxia mimetics cobalt (Co) and desferrioxamine (DFO). The greatest increase in HIF-1 expression is at 1 mM DMOG; the greatest increase in HIF-2 expression is at 0.5 mM DMOG.

PBS-injected pups (Fig. 4*C*) suggests that the mechanism by which OIR is inhibited in these two conditions is likely to be an activation of HIF during the hyperoxic phase, resulting in prevention of central vascular ablation.

Increased Expression of VEGF and Erythropoietin in the Retina, Kidney, and Liver After Treatment with HIF Activators. HIFs play an important role in the regulation of the expression of a number of genes involved in angiogenesis, such as VEGF and erythropoietin (Epo). To assess the ability of the HIF activator DMOG to increase the expression of VEGF and Epo in the retina, normoxic P7 pups were exposed to DMOG for 6 h and the retinas analyzed by ELISA for the expression of these proteins. HIF-regulated proteins VEGF (Fig. 5 *A* and *C*) and Epo (Fig. 5 *B* and *D*) were upregulated in a time- and dose-dependent manner in the retinas of mice treated systemically with the HIF activator DMOG. Because Epo and VEGF are known to be synthesized in the liver and kidney, we analyzed the concentration of these growth factors in these organs after DMOG and found increases in VEGF (Fig. 5*E*), as well as a more dramatic increase in Epo in both liver and kidney (Fig. 5*F*). DMOG stimulated renal and hepatic Epo synthesis by 150- and 300-fold, respectively, measured in picograms per microgram of tissue. We did not see an increase in VEGF or Epo in brain.

Increased Expression of Hepatic HIF-1 Correlates with Epo Synthesis and DMOG-Induced Stabilization of Hepatic Proteins Encoding the ODD. Although HIF-1 is expressed in the mouse P6 retina, we observed there to be no change in HIF-1α stability in the retina after DMOG injection when analyzed by time and dose-response
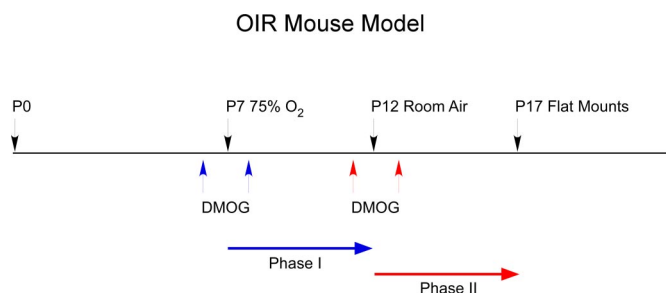
Fig. 2. The mouse OIR model was used to test phase I DMOG injection (blue arrows, at P6 and P8) to phase II DMOG injection (red arrows, P11 and P13). P7 mice are placed in 75% hyperoxia until P12 and then moved to room air until P17, when they are killed.

(Fig. 6*A*). There was also no change in retinal HIF-1α stability after DMOG injection in the retina of mice subjected to hyperoxia for 3 and 6 h after i.p. DMOG injection (Fig. 6*B*). Interestingly, an increase in HIF-1α stability was observed in the liver of mice treated with DMOG (Fig. 6*C*). HIF-2α was stabilized in the kidney after i.p. DMOG injection (Fig. 6*C*). To ensure that the organ-specific HIF-1α stabilization was not just a consequence of sensitivity of the antibody in Western blot analysis, we sought to confirm this finding by using the luciferase-ODD (luc-ODD) transgenic mouse. Hyperoxia promotes the degradation of the HIF-1α subunit by activating oxoglutarate-dependent PHDs that hydroxylate proline residues (Pro-402 and Pro-564) within the ODD of HIF-1α (10, 11). We used the luc-ODD mouse, which contains a transgene composed of the luciferase cDNA fused to the ODD, to track the organs in which DMOG inhibits the activity of PHDs that target HIF-1α ODD. Fig. 6*D* shows a marked increase exclusively in the liver of luc-ODD mouse 6 h after i.p. DMOG injection at both P6 and P8. These data demonstrate that DMOG-mediated increase in HIF-1α stability is liver specific and regulates downstream genes such as VEGF and Epo in a paracrine and endocrine manner to protect the retinal vasculature.

Discussion

This investigation demonstrates the feasibility of preventing ischemia-induced vasoproliferative retinopathy by activating HIF during the causative early hyperoxic phase I of ROP. Activation of HIF under hyperoxic conditions caused an upregulation of proangiogenic molecules Epo and VEGF that likely prevent vascular loss, ischemia, and subsequent proliferative retinopathy. Previous studies have demonstrated a deficiency of Epo during phase I of retinopathy and a protective effect in terms of vascular and neuronal survival after Epo supplementation early in phase I of the disease (16) or in other models of oxygen-induced retinal degeneration (17). Under normal O_2 tension, HIF-α subunits are rapidly degraded via PHD-dependent interactions with the von Hippel-Lindau protein, which is a component of the E3 ubiquitin ligase complex, resulting in degradation of the complex (10). PHD inhibitors are therefore efficient stabilizers and activators of HIF (18). In the hyperoxic environment in the early phase of OIR, proangiogenic molecules are downregulated by O_2-sensing mechanisms. We hypothesized that in addition to Epo there might be a number of vascular growth factors that are regulated by O_2 tension, and therefore activating HIFs early in the disease would allow the upregulation of all these molecules, giving a more robust protective response. In fact, a single dose of the HIF activator DMOG at P7 generated a similar or better vascular survival response than that obtained by four Epo injections of 5,000 U/kg at P6, P8, P10, and P12 (16). Similarly, other investigations have shown limited benefit to directing angiogenesis through the use of VEGF alone (19, 20).

Our results suggest that inhibitors of HIF-α degradation (HIF-1 activators) are potential therapeutic agents that might be beneficial in the treatment and prevention of ROP when administered early in the disease, before proliferative retinopathy has been established. We suspect and caution that administration during the proliferative stage of the disease will have either no effect or might exacerbate the pathology. Morita *et al.* (21) used a conditional HIF-2 knock-down model to determine that HIF-2 was responsible for promoting ROP through Epo expression. They found that mice with reduced expression of HIF-2 did not develop ROP and that i.p. injection of Epo stimulated neovascularization. Our study, like Morita's, confirmed that intervention in phase II using proangiogenic compounds exacerbated OIR.

Our study describes the novel regulation of retinal vascular repair by systemic factors responding to stabilization of HIF-1α
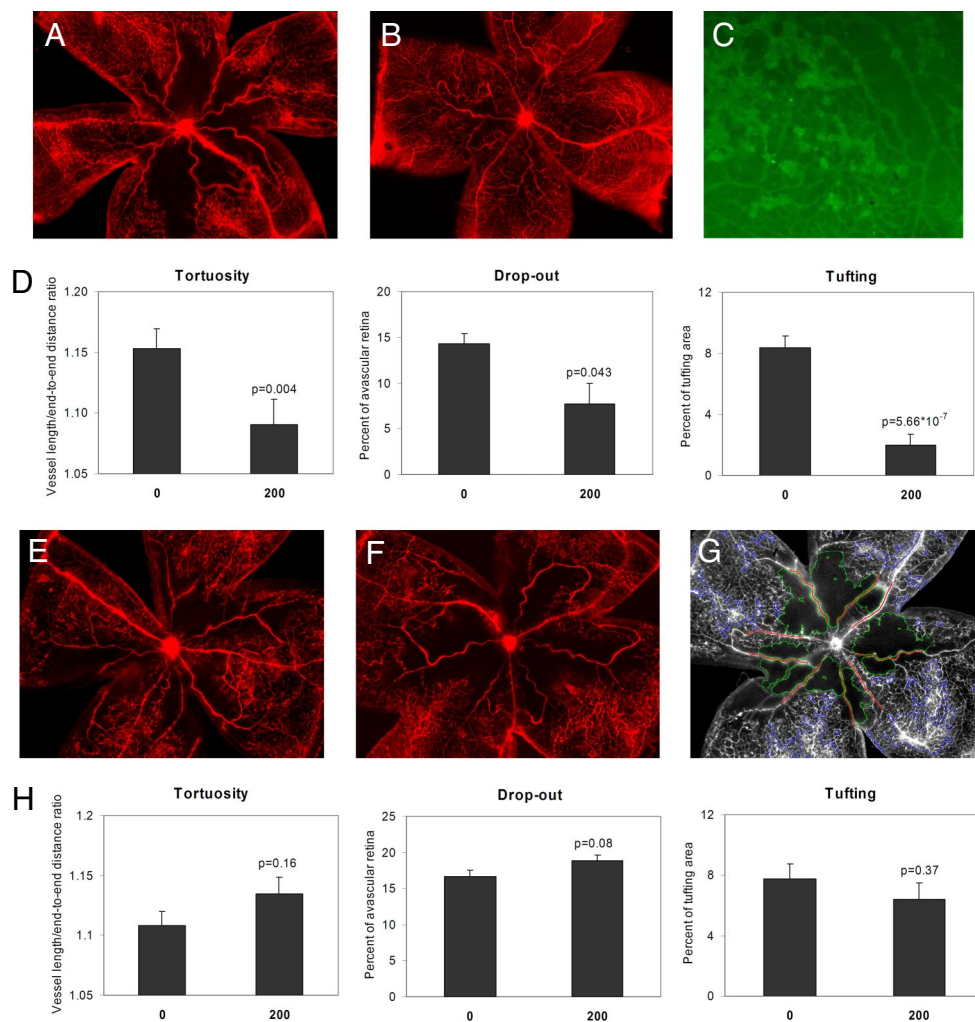
Fig. 3. Inhibition of retinopathy by administration of DMOG in phase I of OIR. Representative flatmounts of OIR from (*A*) mouse injected in phase I with PBS, and (*B*) mouse injected in phase I with DMOG. (*C*) Lectin-stained tufts show new capillary buds induced by the OIR model. (Magnification: ×10.) (*D*) Quantitation of tortuosity, central vascular drop-out, and tufting shows a statistically significant decrease in all three vascular parameters (*n* = 14 animals) in DMOG-injected animals. Representative flatmounts of retinas of OIR from (*E*) mouse injected in phase II with PBS, and (*F*) mouse injected in phase II with DMOG. (*G*) Representative overlay that demonstrates the quantitative analysis performed on flatmounts, obtained from a masked observer using the Image-Pro version 6 program. (*H*) Statistical analysis demonstrates no decrease in all three vascular parameters when DMOG is injected in phase II.

in the liver. It also suggests that there are tissue-specific PHDs that are more susceptible to DMOG inhibition. For example, the affinity of DMOG for PHD-4 suggests that further investigation of this phenomenon should include a survey of tissue-specific expression of PHD isoforms, in addition to a liver-specific conditional HIF-1 knock-out mouse.

In infants with ROP, it has been demonstrated that decreasing the swings in oxygen tension while maintaining oxygen saturation at levels less than 95% early in gestational age drastically reduced the incidence of stage 3 and 4 ROP from 12.5% to 2.5% in four neonatal intensive care units over a 5-year interval (22). Although this investigation shows the utility of decreasing oxygen levels early in neonatal life, this may not be feasible for those infants who require high levels of oxygen for survival. For these infants, our studies determine that perhaps simulating hypoxia chemically by inhibiting PHD during the causative ischemia phase (hyperoxia) of ROP may prevent progression to the proliferative stage of the disease.

HIF activators may protect retinal vessels through local or systemic mechanisms. Although our results suggest that Müller cells are capable of upregulating HIF-1α in response to PHD

inhibitors, it is likely that the majority of HIF response occurs in the liver and/or kidney. The consequential increase in proangiogenic molecules like Epo and VEGF may be a result of systemic synthesis in the liver and kidney, in addition to local production from retinal cells. Critically, the use of small molecules like DMOG enhances the opportunity to regulate therapeutic angiogenesis in the absence of conventional gene therapy (23–25) or stem cell therapy (26). In fact, the overwhelming induction of Epo protein synthesis by DMOG and the reported effects of Epo on mobilization of erythroid precursor cells (27–29) suggest that targeting HIF activation by small-molecule inhibition of HIF-α subunit degradation could be a novel therapeutic approach for the treatment of ROP and other ischemia-induced proliferative retinopathies.

Methods

Murine ROP Model. All animal experiments were performed in strict adherence to the Association for Research in Vision and Ophthalmology Statement for the Use of Animals in Ophthalmic and Vision Research and in accordance with the National Institutes of Health and Cleveland Clinic Animal Research Committee guidelines. OIR was induced in mouse (C57BL6) pups according to a protocol previously established (30). In brief, at P7, rodent pups and their

Fig. 4. Hypoxia preconditioning prevents vascular obliteration in OIR. Flatmounts of retinas at P8 hyperoxia from (*A*) mouse pups exposed to 6% oxygen for 24 h at P6, then subjected to 24 h hyperoxia, as well as (*B*) mouse pups not hypoxic preconditioned. (Magnification in *A* and *B*: *Left*, ×4, *Right* ×10.) Flatmounts of retinas at P10 (during hyperoxia) from (*C*) mouse pups injected with PBS on P6 (phase I) and (*D*) mouse pups injected with DMOG on P6 (phase I). The bar graph demonstrates the quantitative difference in capillary drop-out or avascularity between control (PBS injected) and i.p. DMOG.

Fig. 5. Increased expression of Epo and VEGF after DMOG injections. ELISA for ocular VEGF (*A* and *C*) and ocular Epo (*B* and *D*) demonstrates time and dose–response to i.p. DMOG. Hepatic Epo synthesis (*F*) is dramatically increased by DMOG, even when compared with renal Epo expression. VEGF protein is increased by DMOG in these organs (*E*) but not as much as Epo.

nursing mothers were exposed to hyperoxic conditions (75% oxygen) for 5 days in a Plexiglas incubator with an adjustable oxygen sensor and feedback system (Pro-Ox). On P12, the pups were returned to room-air (normoxic) conditions for 5 days until P17. DMOG (200 μg/g body weight) or control PBS injections were administered i.p. 24 h before hyperoxia (P6) and again after 24 h of hyperoxia (P8). Comparisons between control PBS and test animals were made within the same litter.

Quantification of Vascular Obliteration and Angiogenesis. Animals were anesthetized on day P17 by i.p. injection of Ketanest (1%), Rompun (0.1%), and sodium chloride (0.9%) at a concentration of 0.1 ml/10 g mouse body weight. The heart was exposed through the diaphragm and the left ventricle injected with 0.5 ml of 0.1% Evans Blue dye through a 30-gauge needle. The systemic spread of dye was confirmed by the presence of blue color throughout the skin and tail of the mice. Animals were killed with a lethal dose of intracardiac anesthetic and the eyes enucleated and placed in fresh 4% paraformaldehyde for 2 h. Eye cups were dissected and retinal flatmounts created and examined under fluorescent microscopy. Images of retinas were acquired using a Nikon Microphot-2 fluorescent microscope. Images were acquired with a cooled CCD camera (SPOT-2). For quantitative analysis of drop-out area (area of avascular regions in the center of the retina), vascular tortuosity, and tufting, retinal images were batch processed using a customized macro and algorithms generated in Image-Pro Plus 6.1 (Media Cybernetics). Briefly, each image was converted to grayscale and thresholded (automated histogram search) to determine total retinal tissue area. A circular region of interest (ROI) of a predefined diameter was placed on each image, and the user was prompted to move this ROI to the center of the retina. All pixels outside of this ROI were then masked out (converted to black). Similarly, to exclude contribution of

oversaturated pixels in the center of the retina to any analyses, another, smaller ROI was placed on the masked image for the user to move and resize around the optic nerve. For analysis of drop-out area, pixels within this smaller ROI were converted to white (gray value of 255), and a spectral filter was applied to enhance appearance of large vessels (>50-pixel width). The resultant images were thresholded to create binary masks—grouping vessels in close proximity using a morphologic ''closing'' filter (11 × 11 kernel, four passes). Finally, empty regions within these masks (black, avascular regions) with an area greater than 5,000 pixels were counted and summed. Percentage drop-out was calculated as total drop-out area divided by total retinal area for each image. To determine tortuosity of large vessels emanating from the optic nerve, the previously masked, grayscale images were median filtered to remove noise and contributions of small vasculature. Large vessels within these smoothed images were then segmented using a combination of intensity, length, and aspect ratio filter ranges (in this case the smaller ROI around the optic nerve was filled with black pixels). Extracted vessels were then skeletonized to produce one-pixel-width medial lines and pruned to remove branches. Finally, for each vessel the tortuosity, calculated as the path-length distance divided by the straight line (end-point to end-point) distance, was determined and exported to Excel (Microsoft). Last, for determination of retinal tufting, the ROI first applied to the original grayscale image was again used; however, rather than masking away pixels outside this ROI, these pixels were retained, and pixels within the ROI were removed (converted to black). Because tufting is assumed to occur near the periphery of the retina, this masking step was necessary for removal of pixel contributions near the optic nerve. For segmentation of tufts, these masked images were median filtered to remove noise; objects of similar intensities were grouped using morphologic ''closing'' operations (7 × 7 kernel, two passes). The resultant images were segmented using intensity and size exclusion criteria to determine total tufting area. As with drop-out, percentage tufting was calculated by dividing total tufting area by total retina area. Finally, as a means to verify analysis accuracy, masks of segmented tufts, segmented drop-out areas, and vessels included in tortuosity measurements were converted to edges (Sobel filtered), pseudocolored, and superimposed on the original, unmasked grayscale image.

Each dose of DMOG had an $n = 14$ for phase I (28 eyes) and $n = 9$ (18 eyes) for phase II injections; control animals were equal in number to test animals for each.

Fig. 6. Analysis of HIF-1,2 expression. (A) Western blot of ocular HIF-1α shows no dose or time response to DMOG. Western blot of both retina and total eye lysate from the P6 mouse using four different commercial antibodies to HIF-2α showed no trace of this protein in the P6 retina or whole eye lysate (data not shown). The lack of change in HIF-1α stability was also noted in hyperoxia at 3 h and 6 h after DMOG injection, shown in B. On the other hand, (C) hepatic HIF-1α and renal HIF-2α demonstrated increased stability after DMOG injection. To confirm this finding, the luciferase–oxygen degradation fusion protein transgene (luc-ODD) was used to identify luminescence and hence stability of proteins containing the ODD after i.p. DMOG injection. At P6, (D) DMOG injection clearly demonstrates stabilization of hepatic luc-ODD in comparison with eye and brain, matching the Western blot results in A, B, and C. Taken together, the ELISA, Western blot, and luc-ODD analysis strongly correlate to suggest that the P6 mouse liver is a target of i.p. DMOG, and it is the liver that may protect the retinal vasculature once DMOG stimulates hepatic HIF-1α stabilization.

Western Blot Analysis. Mice at P6 24 h before hyperoxia were injected with DMOG prepared as an aqueous solution (10 mg/ml) for dose–response (0, 125 μg/g, 250 μg/g, and 500 μg/g) and time course (0, 3 h, 6 h, and 9 h). Eye cups were prepared by removing the cornea, iris, and lens. The anterior lobe of the liver, the right kidney, and temporal lobe of the brain were obtained at for each dose and time point. All tissues were placed in RIPA buffer (200 micro-

liters per 50 mg of tissue, pH 7.0) containing protease inhibitors, disrupted using a tightly fitted pestle, and centrifuged to remove particulate matter. A bicinchoninic acid protein assay (Pierce, Rockford, IL) was used to measure protein concentration. Lysates were subjected to 4%–20% SDS-PAGE and electro-transferred to PVDF membrane for immunoblotting. Membranes were blocked with 5% nonfat dried milk in Tris-buffered saline (TBS) and 0.1% Tween-20 and probed with anti-HIF-1α (Santa Cruz Biotechnology), HIF-2α (Novus) antibody, and after washing three times for 10 min with TBS and 0.1% Tween-20 and secondary antibody hybridization, exposed by chemiluminescence (Western Lightning, Perkin–Elmer). $n = 6$ for each Western blot.

Müller Cell Western Blot. Müller cells (MIO-M1) were kindly provided by Dr. G.A. Limb (Institute of Ophthalmology, London, United Kingdom) and plated at a density of 10^5 cells per 100-mm plate in DMEM supplemented with 400 mM glutamine and 10% FCS (31). Before stimulation, cells were placed in serum-free media for 24 h. A dose–response of DMOG was constructed from an aqueous stock solution (10 mg/ml). Cells were treated with media alone, cobalt chloride, and desferrioxamine as positive controls, and various doses of DMOG. Cells were harvested in each particular experiment by scraping them into 2 ml chilled PBS and pelleting them in a 15-ml conical tube at 500 rpm for 5 min. Cell lysates were made by directly resuspending cells in 2× sample buffer with 1 mM DTT. Lysates were subjected to 4%–20% SDS-PAGE and electro-transferred to PVDF membrane for immunoblotting. Membranes were blocked with 5% nonfat dried milk in TBS and 0.1% Tween-20 and hybridized with anti-HIF-1α (BD Transduction Laboratories) and anti-HIF-2α antibody (Novus), and after washing and secondary antibody hybridization, exposed by chemiluminescence (Western Lightning; Perkin–Elmer).

VEGF and Epo ELISA. Fifty microliters of tissue lysates (adjusted to 1 mg/ml) was added 1:1 to sample diluent provided by the manufacturer of mouse VEGF or Epo colorimetric ELISA (R&D Systems). VEGF or Epo measurements were performed according to the manufacturer's instructions. $n = 6$ for each measurement.

Luciferase Assay. The GT(ROSA)26sor/luc mouse (Jackson Laboratories) were received as timed pregnant females and breeding pairs. Pups were injected i.p. with 200 μg/g body weight DMOG dissolved in PBS at a stock concentration of 10 mg/ml. Eye, brain, kidney, and liver were isolated from at least three pups each litter and compared with an equal number of PBS-injected control pups. Each luciferase experiment was repeated three times. Lysates were prepared in Glo lysis buffer (Promega) and 100 μg of protein mixed with 100 μl of Bright Glo (Promega). Luminescence was measured using a Wallace 1420 Victor2 (Perkin Elmer).

Statistical Analysis. The size of the difference between the means of values obtained by a masked observer using Image-Pro analysis and absorbance used in the ELISA were compared with the standard error of that difference using the Student's t test. The probability of error associated with rejecting the hypothesis of no difference between treated and untreated groups as a two-tailed probability was calculated and is supplied in the figures.

1. Alon T, *et al.* (1995) Vascular endothelial growth factor acts as a survival factor for newly formed retinal vessels and has implications for retinopathy of prematurity. *Nat Med* 1:1024–1028.
2. Pierce EA, Foley ED, Smith LE (1996) Regulation of vascular endothelial growth factor by oxygen in a model of retinopathy of prematurity. *Arch Ophthalmol* 114:1219–1228.
3. Geisen P, *et al.* (2008) Neutralizing antibody to VEGF reduces intravitreous neovascularization and may not interfere with ongoing intraretinal vascularization in a rat model of retinopathy of prematurity. *Mol Vis* 14:345–357.
4. Kim JH, Yu YS, Shin JY, Lee HY, Kim KW (2008) Deguelin inhibits retinal neovascularization by down-regulation of HIF-1alpha in oxygen-induced retinopathy. *J Cell Mol Med*, in press.
5. Brafman A, *et al.* (2004) Inhibition of oxygen-induced retinopathy in RTP801-deficient mice. *Invest Ophthalmol Vis Sci* 45:3796–3805.
6. Semenza GL (2006) Regulation of physiological responses to continuous and intermittent hypoxia by hypoxia-inducible factor 1. *Exp Physiol* 91:803–806.
7. Semenza GL, Nejfelt MK, Chi SM, Antonarakis SE (1991) Hypoxia-inducible nuclear factors bind to an enhancer element located 3′ to the human erythropoietin gene. *Proc Natl Acad Sci USA* 88:5680–5684.
8. Jiang BH, Rue E, Wang GL, Roe R, Semenza GL (1996) Dimerization, DNA binding, and transactivation properties of hypoxia-inducible factor 1. *J Biol Chem* 271:17771–17778.
9. Semenza GL, Wang GL (1992) A nuclear factor induced by hypoxia via de novo protein synthesis binds to the human erythropoietin gene enhancer at a site required for transcriptional activation. *Mol Cell Biol* 12:5447–5454.
10. Ivan M, *et al.* (2001) HIFalpha targeted for VHL-mediated destruction by proline hydroxylation: Implications for O2 sensing. *Science* 292:464–468.
11. Jaakkola P, *et al.* (2001) Targeting of HIF-alpha to the von Hippel-Lindau ubiquitylation complex by O2-regulated prolyl hydroxylation. *Science* 292:468–472.
12. Ratcliffe PJ (2006) Understanding hypoxia signalling in cells—a new therapeutic opportunity? *Clin Med* 6:573–578.
13. Mole DR, *et al.* (2003) 2-oxoglutarate analogue inhibitors of HIF prolyl hydroxylase. *Bioorg Med Chem Lett* 13:2677–2680.
14. Schlemminger I, *et al.* (2003) Analogues of dealanylalahopcin are inhibitors of human HIF prolyl hydroxylases. *Bioorg Med Chem Lett* 13:1451–1454.
15. Ozer A, Bruick RK (2007) Non-heme dioxygenases: Cellular sensors and regulators jelly rolled into one? *Nat Chem Biol* 3:144–153.
16. Chen J, Connor KM, Aderman CM, Smith LE (2008) Erythropoietin deficiency decreases vascular stability in mice. *J Clin Invest* 118:526–533.
17. Rex TS, *et al.* (2004) Systemic but not intraocular Epo gene transfer protects the retina from light- and genetic-induced degeneration. *Mol Ther* 10:855–861.
18. Kaelin WG, Jr (2005) The von Hippel-Lindau protein, HIF hydroxylation, and oxygen sensing. *Biochem Biophys Res Commun* 338:627–638.

19. Baumgartner I, et al. (2000) Lower-extremity edema associated with gene transfer of naked DNA encoding vascular endothelial growth factor. *Ann Intern Med* 132:880–884.

20. de Muinck ED, Simons M (2004) Re-evaluating therapeutic neovascularization. *J Mol Cell Cardiol* 36:25–32.

21. Morita M, et al. (2003) HLF/HIF-2alpha is a key factor in retinopathy of prematurity in association with erythropoietin. *EMBO J* 22:1134–1146.

22. Chow LC, Wright KW, Sola A (2003) Can changes in clinical practice decrease the incidence of severe retinopathy of prematurity in very low birth weight infants? *Pediatrics* 111:339–345.

23. Date T, et al. (2005) Expression of constitutively stable hybrid hypoxia-inducible factor-1alpha protects cultured rat cardiomyocytes against simulated ischemia-reperfusion injury. *Am J Physiol Cell Physiol* 288:C314–C320.

24. Asikainen TM, et al. (2005) Activation of hypoxia-inducible factors in hyperoxia through prolyl 4-hydroxylase blockade in cells and explants of primate lung. *Proc Natl Acad Sci USA* 102:10212–10217.

25. Milkiewicz M, Pugh CW, Egginton S (2004) Inhibition of endogenous HIF inactivation induces angiogenesis in ischaemic skeletal muscles of mice. *J Physiol* 560(Pt 1):21–26.

26. Ritter MR, et al. (2006) Myeloid progenitors differentiate into microglia and promote vascular repair in a model of ischemic retinopathy. *J Clin Invest* 116:3266–3276.

27. Bahlmann FH, et al. (2004) Erythropoietin regulates endothelial progenitor cells. *Blood* 103:921–926.

28. Heeschen C, et al. (2003) Erythropoietin is a potent physiologic stimulus for endothelial progenitor cell mobilization. *Blood* 102:1340–1346.

29. Satoh K, et al. (2006) Important role of endogenous erythropoietin system in recruitment of endothelial progenitor cells in hypoxia-induced pulmonary hypertension in mice. *Circulation* 113:1442–1450.

30. Smith LE, et al. (1994) Oxygen-induced retinopathy in the mouse. *Invest Ophthalmol Vis Sci* 35:101–111.

31. Hollborn M, et al. (2004) Characterization of the basic fibroblast growth factor-evoked proliferation of the human Müller cell line, MIO-M1. *Graefes Arch Clin Exp Ophthalmol* 242:414–422.

MEDICAL SCIENCES